The International Journal of Engineering and Science (IJES)
|| Volume || 12 || Issue || 1 || January || Pages || PP 12-21 || 2023 ||
ISSN (e): 2319-1813 ISSN (p): 20-24-1805

# Friction Stir Welding in Austenitic 316L and Martensitic/Ferritic F82H Steels Joints: Effect on Mechanical Properties and Microstructure

Víctor Manuel Alcántara
[1]*Department of Mechanics and Energy,Materials and Processes,National university of Trujillo, Perú.*
*Corresponding Author:*[1]*Víctor Manuel Alcántara*

**----------ABSTRACT----------**
*The friction stir welding (FSW) process was applied in two dissimilar materials: 316L stainless steel and F82H structural steel, using butt joints to observe its effects on microhardness, mechanical properties and microstructure. Plates of 600x200x4mm$^3$ were used to measure the microhardness profile on the Vickers HV0.5 scale, following the ASTM E-92 standard. For the tensile tests, samples were manufactured according to the ASTM E8M standard. These tests were carried out in a 10 Tn Universal Instron Machine. The welding parameters were: Joint M1= F82H (AS) - 316L (RS) (300rpm and 75mm/min); Joint M2 = 316 (AS) – F82H (RS) (300 rpm and 75 mm/min); Joint M3= F82H (AS) - 316L (RS) (400rpm and 100mm/min); Joint M4 =16 (AS) – F82H (RS) (400 rpm and 100 mm/min). Welding tests were performed on a vertical milling machine with 3° head inclination. The microstructure was revealed at optical level and electronic level(SEM), with an EDS assay.to distinguish the SZ, TMAZ and HAZ zones. It was found:As the rotation speed and linear speed of the joint increase, the hardness of the welded joint increases too. The maximum values of hardness and tensile properties (YS, UTS, ε) are presented in the M3 joint. The highest efficiency of the welded joint was 87% and it was presented in sample M3. The maximum impact resistance (27.5J) was also presented in the M3 sample. There was an exchange of materials around the zone (ST), due to the material removal process in addition to the diffusion process at the interface, due to the high temperature in this zone. The microstructure in the zone (ST) of the joints showed: In the F82H steel martensite and ferrite, and in the 316L zone it was totally austenite.*
***KEYWORDS;*** *Friction Stir welding; welding parameters; mechanical properties; microhardness*

---

Date of Submission: 28-12-2022 Date of Acceptance: 08-01-2023

---

## I. INTRODUCTION

Friction stir welding (FSW) is a new solid-state welding joining technique that has become a powerful solid-state joining process for materials. This process includes three phases that are extrusion, shearing and consolidation of material at high temperature[1,2]. This process has the advantage of not using consumable electrodes; temperatures lower than the melting temperature are used, they are easier to weld and have a more refined microstructure. Since the electrodes not emit gases, it is considered a clean process, not harmful, nor pollute the environment; that is, it is an ecological welding process[3]. This new welding technique has many applications in various industrial sectors: naval, automotive, aerospace and others. In decades past, this type of FSW welding was generally applied to join light metal alloys, especially aluminum, magnesium and/or copper [4, 5]. Currently it is also used in the union of low carbon and stainless steels, and low alloy steels with good mechanical resistance.

FSW process can be performed with the help of a conventional or CNC vertical milling machine. Through a cone attached to the mandrel, a pin is connected as a tool, which is then rotated and immersed within the edges of the base metal (BM) plates and subsequently given a determined linear speed. The tool carries out the following functions: 1) Heat the work piece by friction, up to a temperature that does not cause fusion; 2) Remove the material from the union zone to achieve coalescence, and by diffusion produce the union [6]. During the stirring process, the material undergoes intense plastic deformation, which results in the generation of fine recrystallized grains, which allow obtaining good mechanical properties. The FSW joints have three affected zones: 1) Central agitation or SZ zone; 2) Another zone adjacent to the first or thermomechanically affected zone (TMAZ) and 3) The last zone, that is furthest from the center, where it only suffers thermal and non-mechanical effects called, Heat Affected Zone (HAZ) [7].

FSW process performs well, when is applied to light materials; however, when they are applied to hard and resistant materials such as steels, it becomes more difficult, due to wear and degradation of the tool [8]. This degradation can be attributed to the high heat generated reaching temperatures ~ 1200 °C, in addition to the high

stresses that occur during the process[9]. Many studies report that FSW welded joints in steels have better performance compared to fusion welds. It is believed that this improvement is due to the formation of a microstructure composed of very fine grains in the zone (SZ). However, other works report a wide variety of microstructures in the SZ zone. For example, if the process is applied to low carbon steels, the microstructure is a mixture of fine-grained ferrite and pearlite[10]When applied to medium and/or high carbon steels, the microstructure is a mixture of ferrite, pearlite, martensite and/or bainite, depending on the carbon content and the maximum temperature reached by the process[11, 12], aspects, which demonstrate that the full phenomenon of the FSW process is still not fully understood.

An extensive background review related to the subject has been carried out, but the literature on the application of FSW in stainless steels is still scarce. C. Meran et al. [13] report that the microstructural evolution of steels during FSW is more complicated than that of aluminum alloys due to transformation, recrystallization and grain growth at a temperature of 1000 °C or higher. These changes are significantly influenced by the composition of the alloy. A.P. Reynolds et al. [14], report that for austenitic stainless steels, an equiaxed grain structure develops within the SZ zone with significant grain refinement up to an order of magnitude relative to the base metal. Other studies report that the TMAZ zone, typically observed in FSW aluminum, is not evident in steels due to transformations during thermal cycling[15, 16, 17]. However, Park et al. [18] identified the existence of the TMAZ zone in FSW 304 and 316L, further adding that this zone is characterized by a recovered microstructure, while R. Johnson and P. Threadgill [19] observed evidence of partial recrystallization in the TMAZ zone of FSW 304L and 316L., A. Tiwari et all [20]., studied the effect of the location shape, tool clearance and its speed of rotation, on the mechanical properties of the FSW dissimilar weld: SS AISI 304 -Steel simple medium carbon. It was found that the Charpy impact toughness is lower than for the base materials: YS yield strength and UTS maximum strength increase with increasing rotational speed. The microstructure of the joint revealed a complex mixture of tungsten-rich banded materials.D. Sunilkumar et al.[21] report about the role played by the rotation speed of the tool in the microstructure and its effect on the hardness of 2.25Cr–1Mo (P22) steel welded by FSW with AISI 316LN steel. The martensitic transformation was found on the P22 steel side due to the maximum temperature found. The average hardness of that martensitic structure on the P22 steel side was 405 HV0.2; This phenomenon indicates that a post weld heat treatment is mandatory for dissimilar FSW welds. G. Guo and Y. Shen [22] experimented with dissimilar FSW joining with AISI 304 - AISI 430 stainless steels, using a stepped butt joint configuration. The primary objective was to study the effect of the size of the pin with respect to the flow of material removed. The evolution of the microstructure and mechanical properties of the joint was observed. The results indicate that the flow of material tends to improve with the reduction of the width of the pin; However, when the width of the pin is reduced to 1 mm, the degree of mixing of the base metals in the stirring zone worsens due to the lack of smoothness of the softened metal. The joint made with a pin width of 2 mm presented a flow pattern with several directions in different regions of the SF zone; pattern formed by a mixed structure of austenite and ferrite with various grain sizes.Cao et al. [23] reports the behavior of similar plates welded from 2507 duplex stainless steel using FSW. Two rotary speeds were used: 400 and 800 rpm and a constant linear speed of 60 mm/min. The result was successful for the joint welded at 800 rpm while the joint welded at 400 rpm presented defects. Although the microstructures were similar in the SZ, the direction change of the α/γ fiber structureswere different. These microstructure changes led to a higher YS, and a UTS compatible with the MB, but the Elongation decreased considerably, mainly due to the changeof α/γ fiber structures, being detrimental to the union.

The purpose of this work is to investigate the mechanical properties, hardness and microstructure of welded joints of two dissimilar steel plates: Stainless steel, AISI 316L with another low alloy chrome biphasic steel F82H using the FSW process.

## II. MATERIALS AND METHODS

### 2.1. Materiales.

Se utilizaron placas de3.5 mm de espesor dos tipos de aceros 1) El acero inoxidable austenítico AISI 316L y 2) Acero F82H que es un aceroestructural al Cr, bifásico ferrítico/martensítico de baja activación. El término de baja activación significa que estos materiales son adecuados para ser usados en ambientes expuestos a todo tipo de radiación. La composición química se puede observar en la tabla 1.

**Tabla 1** Composición Química de los materiales (w%)

| Acero | C | Cr | Ni | Mo | Mn | V | W | Ta | Si |
|---|---|---|---|---|---|---|---|---|---|
| **316L** | 0.10 | 9.2 | 0.02 | - | 0.47 | 0.21 | 1.0 | 0.087 | 0.12 |
| **F82H** | 0.02 | 16.58 | 12.07 | 2.02 | 0.8 | - | - | - | 0.28 |

### 2.1. Experimental Methodology.

For this purpose; Initially rectangular plates or coupons had to be cut from the supply sheets. The coupons for both types of steel were machined with the same dimensions: 300 mm long, 100 mm wide, and 3.5 mm thick, and were then used as base material (BM) for the joints. Each joint consisted of a plate of F82H and another of 316L, to be later butt welded.

❖ **Tensile test**

After the plates were welded, butt-joining the two halves of dissimilar materials, the arrangement in which the tensile specimens would be made was traced, following a transverse arrangement to the interface of the welded joint. The machining of these specimens was carried out transversally and the dimensions of each one of them were obtained, as established in the norms for tensile tests, following the ASTM-EM8 standard, for welded specimens of prismatic section and small thickness.

❖ **Impact tests: Charpy.**

The specimens were machined, following the ASTM E 23 – 93a standard, and the dimensions are standardized within the norm. For the preparation of these specimens, plates of (1/2" = 12.7 mm) had to be used to then machine coupons with dimensions of 300mmx 100mm x 12mm thick and they were welded by FSW, following the same previous methodology. The cut was made transversally to the direction of the welded joint and the dimensions are standardized (55mmx10mmx10mm), with a 10mm deep x 45° notch located in the center of the specimen.

**II.4.2. FSW Welding tests.**

These tests were carried out using a vertical milling machine to which a clamping and anchoring device was attached as shown in figure 1. The tool used corresponds to a standardized model. It was the model: *BOND STIR T50*. They are tools made of WC tungsten carbide with BCN cubic boron nitride removal pin. The tool was tilted 3° from the vertical for better performance.

**III.4.2.1.Parameters Used in the FSW welding process.**

The parameters were taken according to the specialized technical literature. They are found in Table 2 with their respective nomenclature.

Table2. Nomenclature of welded joints and parameters used.

| Nomenclatura | Descripción | V. Rotación (rpm) | V. Lineal (mm/min) |
|---|---|---|---|
| **M1** | **F82H(AS) - 316L (RS)** | 300 | 75 |
| **M2** | **316L (AS) - F82H (RS)** | 300 | 75 |
| **M3** | **F82H(AS) - 316L (RS)** | 400 | 100 |
| **M4** | **316L (AS) - F82H (RS)** | 400 | 100 |


**Figure 1.** Experimental scheme of FSW welding process.

## III. RESULT AND DISCUSION

### 3.1. Microhardness profiles.

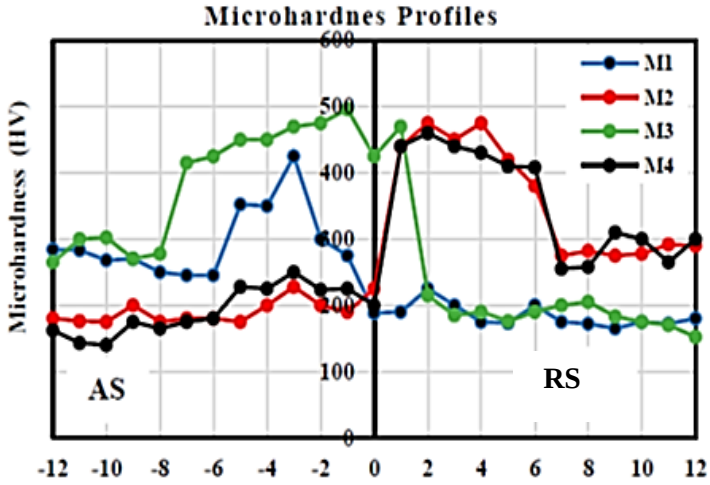


**Figure 2.**Graph showing the micro hardness profiles of all FSW welded joints

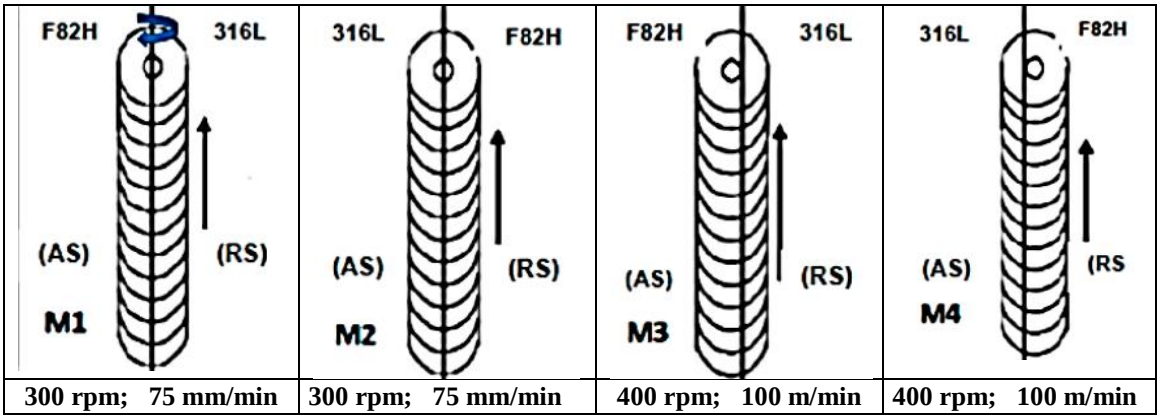


**Figure 3.**Scheme of welding procedure for each sample. The direction of rotation is observed, which is the same for all of them, and the longitudinal movement of the joints, indicating the AS and RS zones.

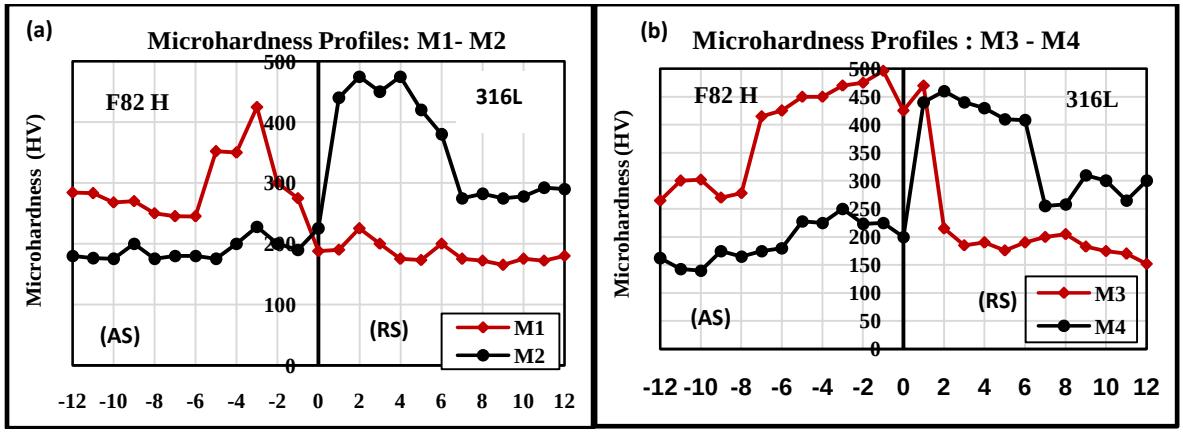


**Figure4.** (a) Microhardness profiles of welded joints M1-M2; (b) Microhardness profiles of joints M3-M4

Figure 2 shows the microhardness profiles of all samples. Irregular profiles are observed, without any symmetry and with a tendency to increase when approaching the interface. The maximum hardness peak (496 HV) is

found at the M3 joint (400 rpm, 100 mm/min), located 1 mm to the left of the interface and the minimum value (188HV) is found at the M1 joint ( 300 rpm, 75 mm/min) located on interface.

These results show that an increase in the speed of rotation and advance bring about higher values in the hardness of the joint, as observed in the profiles of figure 4; in accordance with the parameters shown in Figure 3. On the other hand; the profiles indicate that for both materials that make up the joint, the hardness values are higher than their corresponding base materials (MB). A random fluctuation in hardness values is also observed in the zone (SZ). This phenomenon is due to the mixture of materials in the joint area, as can be seen in figures 7 and 8. For the four types of joint; in the left zone we have dispersion of material corresponding to the right zone and vice versa. The cause can be attributed to two phenomena: 1) First, to the same mechanical process of agitation; and 2) Secondly, the diffusional effect, due to the high temperature produced in the SZ zone, which reaches recrystallization temperatures close to melting temperatures.

The micro hardness profiles are not symmetrical, not even when the order of placement of the plates is reversed. Although this inversion affects the hardness peaks little, but it does affect the hardness obtained in the very center of the bead, and the hardness coverage in the TMAZ and HAS zones (thermomechanically affected zones and heat-affected zone). This variability is explained by the tangential speed with which the pin removes the material. The plate located in AS (advancing side) is the one where the tangential velocity of the pin goes in the same direction as the advance velocity of the joint. The AR zone (retreating side) indicates the opposite; that is to say, the speed of the pin goes against the speed of advance, producing a braking in the removal of the material. This difference in stirring speed is the main cause for a symmetry in the profile not to occur; something very typical in FSW welds; which almost does not happen when using fusion welding.

### 3.2Mechanical Properties.

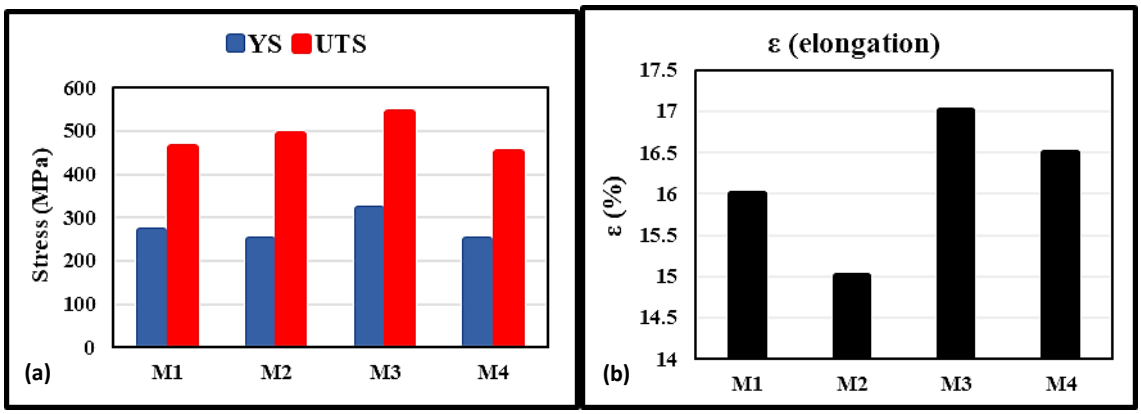


**Figure5**, (a) YS (MPa) Yield Limit Values, and UTS Maximum Strength (MPa), found in the tensile tests, for each of the FSW welded samples; (b) Maximum elongation (%) for each of the samples.

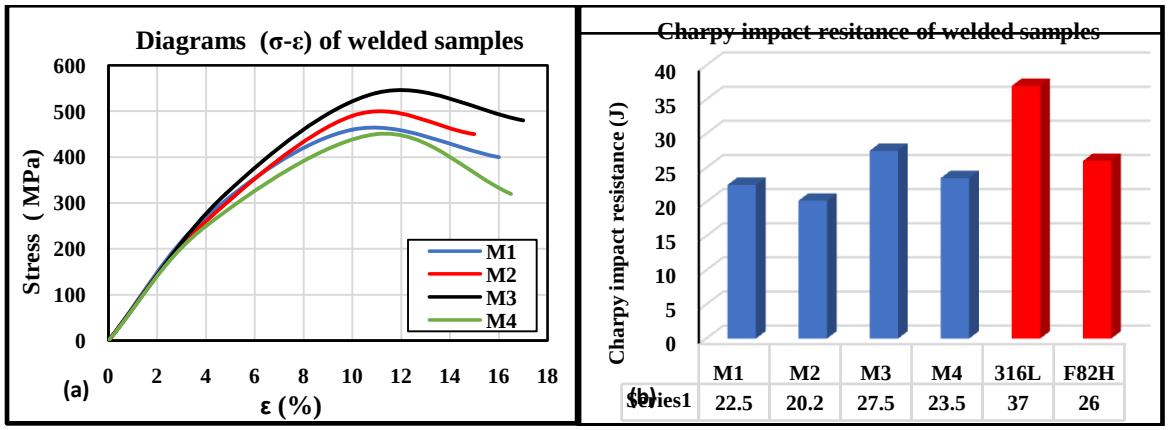


**Figure6**, ((a) Stress-Strain diagrams for the welded samples; (b) Graph showing the variation of results obtained in the Charpy test. The results of the supply samples are in red.

The results of the tensile mechanical properties are shown in Figure 5 (a,b). The maximum values of the Tensile properties (YS, UTS, ε) are presented in the M3 joint [ F82H (AS) – 316L (RS)]. The YS has a maximum (320 MPa) and minimum (250 MPa) value for M4. The UTS presents a maximum value (540 MPa)

for M3 and a minimum (450 MPa) for M4. The elongation "ε" its maximum value is 17% for M3 and minimum 15% for M2. It can be seen that the graphs show oscillating values at the joints, but always maintaining a maximum peak for sample M3. Figure 6(a) shows the curves (σ-ε) for the four types of joints. What stands out is that it indicates that the elastic limit has remained constant. On the other hand, the M3 joint, which presents the highest UTS value, in turn presents the highest elongation or ductility; phenomenon that is not observed in the other three joints (M1, M2 and M4), where an increase in mechanical resistance is accompanied by a slight decrease in ductility. Therefore; we can affirm that; The change in welding parameters has little effect on the ductility of the samples welded by FSW. Besides; According to the values shown, a maximum welding efficiency is reached (87%), with respect to mechanical resistance and corresponds to the M3 joint.

The Charpy Impact Strength results are shown in Figure 6(b). The maximum impact resistance (27.5J) of the welded joints was obtained in sample M3. However, this value is slightly higher than the base material F82H steel (26J) and less than corresponding to the base material 316L (37J). The trend of the impact values of the samples is irregular. In all cases, the impact values of the samples are lower than those corresponding to the base metal; noting a large deviation compared to 316L steel. This is explained by the composition of the joint materials. Besides, due to the presence of austenite at room temperature, 316L austenitic stainless steel has a much lower ductility than F82H martensitic/ferritic steel, which presents brittle martensite at room temperature.

**3.3 Macrophotographs the cross sections of the joints.**

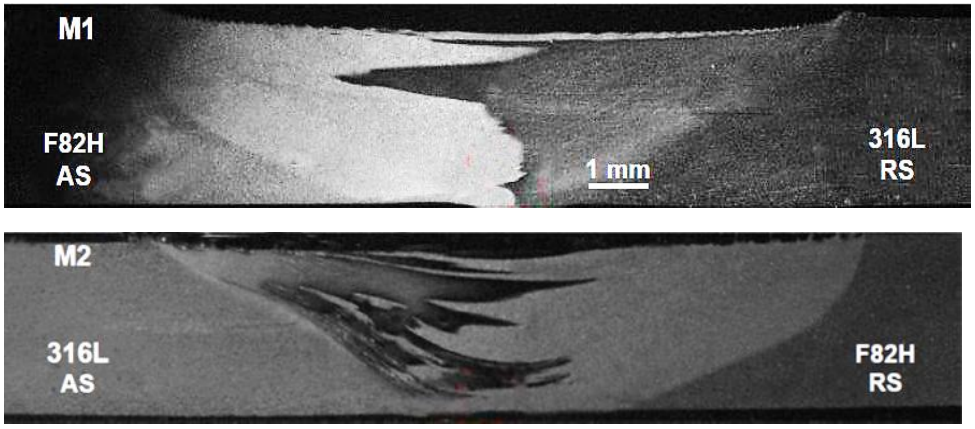


**Figure7.** Macrophotographs of the welded samples: M1 and M2, using the FSW method (300 rpm, 75 mm/min)

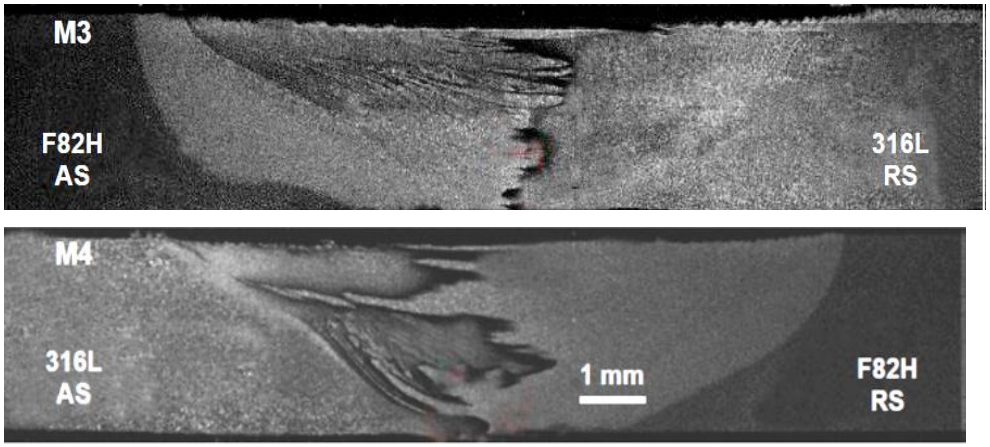


**Figure8.** Macrophotographs of the welded samples: M3 and M4, using the FSW method. (400 rpm, 100 mm/min).

Figure 7 shows the macrophotographs of the welded samples: M1 and M2 with parameters: 300 rpm, 75 mm/min. The exchange of materials around the central zone or zone of agitation (ST) is clearly observed. Figure 8 shows the Macrophotographs of the welded samples: M3 and M4, with parameters: 400 rpm, 100 mm/min. The exchange of materials in the area (ST) is also observed. This exchange of materials is produced by the same agitation process and the diffusion process is also involved due to the friction temperature at the

interface. Diffusion depends on its diffusional coefficient "Do" which is a function of temperature and different for both materials depending on their composition.

**3.3 Microstructure.**

The cross-sectional area of the welded sample M3 has been taken as the microstructure model, as it is the most representative, having obtained the highest mechanical and impact properties. The microstructures shown correspond to the central zone (SZ zone) in three different positions, as shown below.

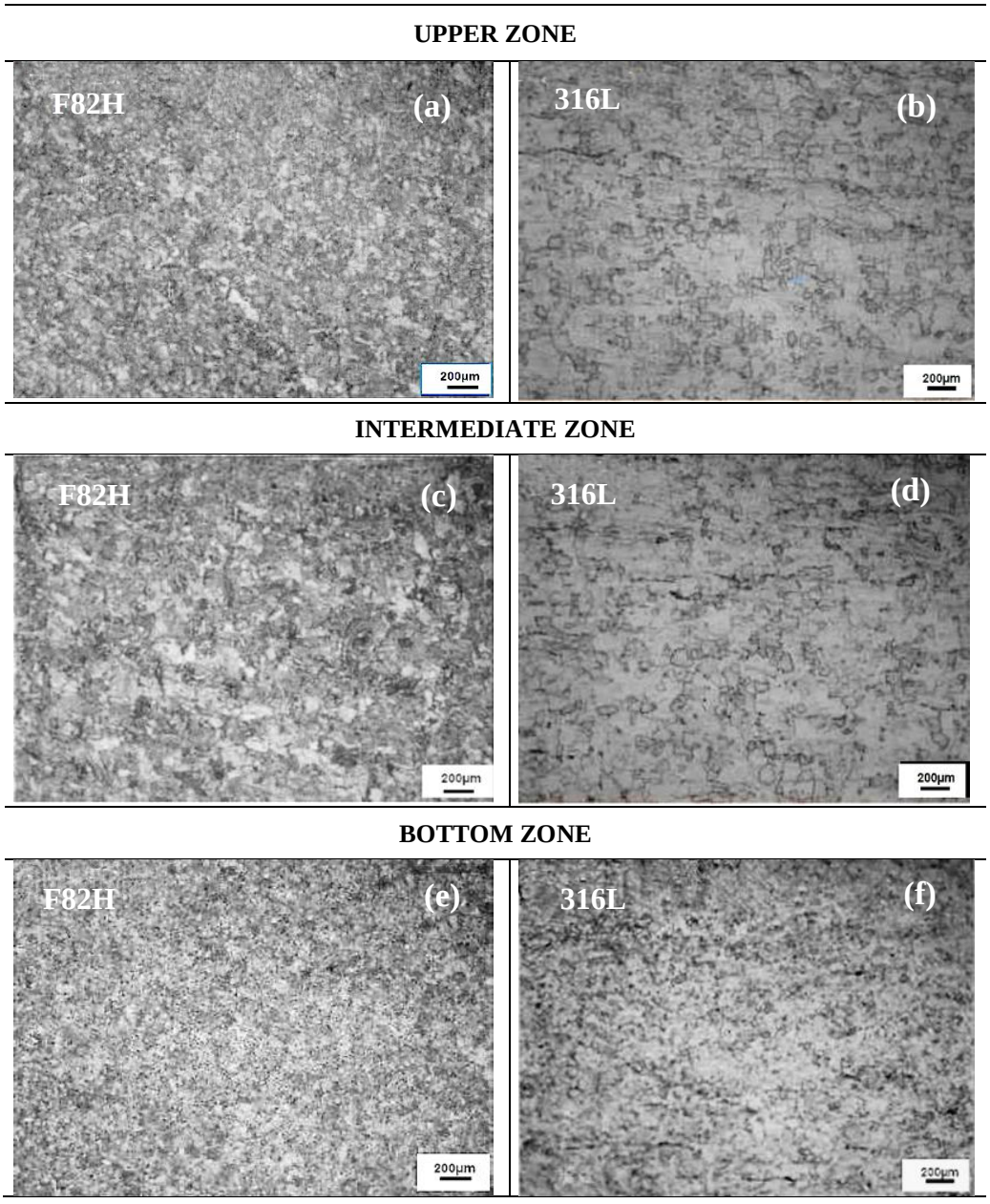


**Figure9.**Optical microstructure of the central zone of the joint (SZ), from sample M3, where a cross section of the interface has been made. a), b) correspond to the surface area of the joint; b) and c) intermediate area of the joint; c) d) lower area of the joint.

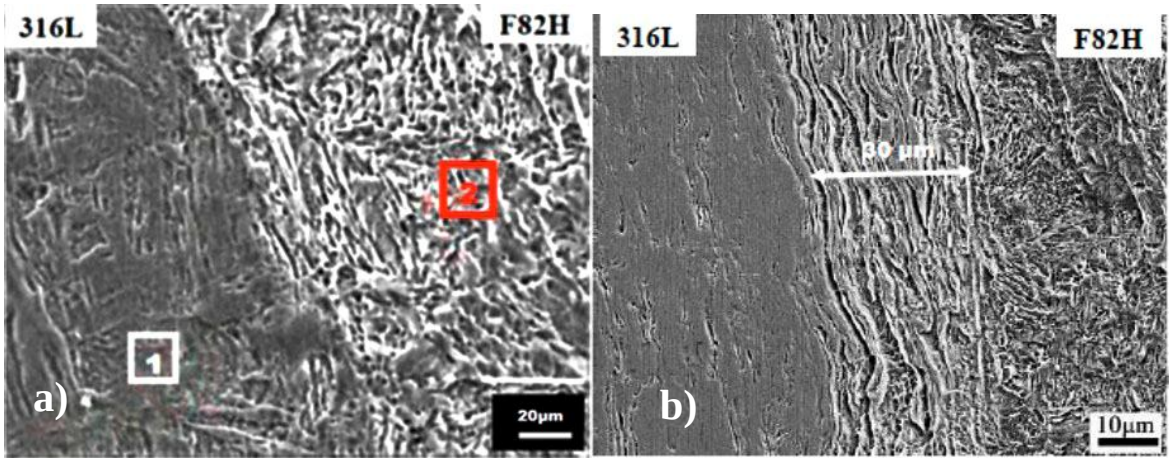


**Figure 10.**(a) SEM microphotograph of the upper area of the M3 sample, where 2 points close to the junction area are analyzed. (b) Larger scale SEM photomicrograph. It can be seen that the bonding zone has an average thickness of 30µm.

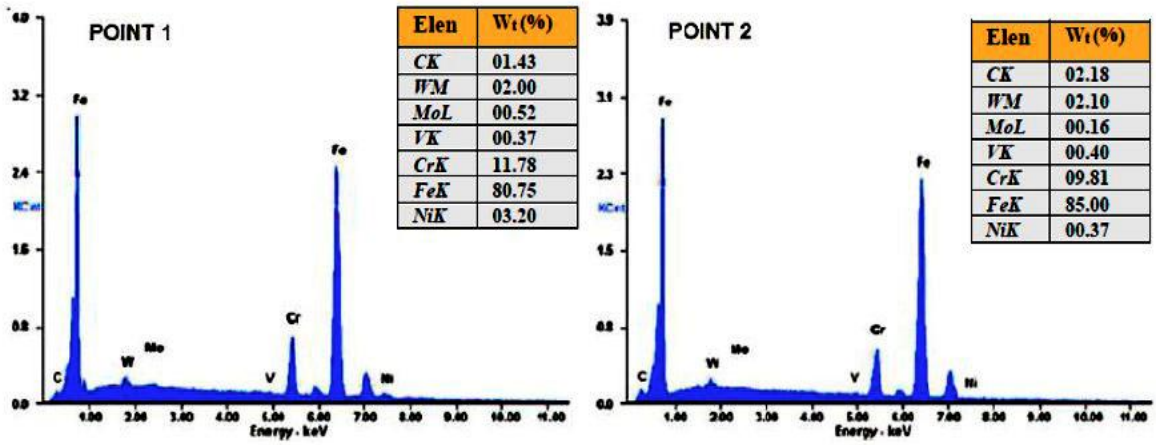


| Elen | Wt(%) |
|---|---|
| CK | 01.43 |
| WM | 02.00 |
| MoL | 00.52 |
| VK | 00.37 |
| CrK | 11.78 |
| FeK | 80.75 |
| NiK | 03.20 |

| Elen | Wt(%) |
|---|---|
| CK | 02.18 |
| WM | 02.10 |
| MoL | 00.16 |
| VK | 00.40 |
| CrK | 09.81 |
| FeK | 85.00 |
| NiK | 00.37 |

**Figure 11.**Results of EDS test applied to the two points indicated in Fig. 9(a).

Figure 9 shows the microstructures of the welded samples, which correspond to the "M3" welded joint. As previously stated, it is the prototype sample, as it is the one that provided the best results regarding mechanical properties. To better visualize the change of structures in the whole zone, three visualization zones have been chosen: Upper, intermediate and lower. The results show; that the microstructure of the ST zone corresponding to the F82H steel consisted mainly of martensite and ferrite, and in the zone corresponding to the 316L steel, it was completely austenite. In the SZ zone of F82H steel; from the top to the bottom of the joint, the grain size first increased and then decreased; the largest grain size was achieved in the middle part. In the SZ zone corresponding to 316L steel, from the top to the bottom the austenite grain size decreased.

It must be taken into account that Ni is the most important alloying element to form and stabilize austenite in steels. At the end of the 316L stainless steel side near the joint interface, the amount of Ni was most likely decreased by diffusional effect and the absence of Ni reduced the stability of the austenite. Therefore, the final Cr and Ni contents provided a favorable composition for the martensitic transformation during the cooling process after welding. This phenomenon would be the justification that explains randomly widely dispersed peak values of hardness and mechanical properties were obtained.

Figure 10a) and 10b) show SEM images of typical microstructures of 316L stainless steel mixed with F82H steel. In the first we observe an almost continuous line and in the second the thickness of the mixture is observed with higher magnifications. The distribution of alloying elements with the two materials becomes more continuous as you approach the center of the joint. This indicates that in addition to the mechanical mixing of the two materials, diffusion of Cr and Ni occurred with a more pronounced trend from 316L stainless steel to F82H steel during the FSW process. The average thickness of the mixed zone of ~30 µm can be seen in detail in Figure 10b).

Figure 11 shows the results of the EDS analysis at the two points indicated in Figure 10a) and found in the two dissimilar materials ~50 µm away from the junction interface. The analysis found that the selected area on the F82H steel side, the Ni content increased to 0.37% by weight. In addition, the Ni Content of the selected area in the 316L stainless steel decreased to 3.20 wt%, which was obviously lower than that of BM-316L (~9.2

wt%). This great difference in concentrations shows that a large amount of Ni in BM-316L has diffused into the matrix of F82H steel.

An aspect that must be taken into account; is that Ni is the most important alloying element for forming and stabilizing austenite in steels. At the edge of the 316L stainless steel side near the bond interface, the absence of Ni reduced austenite stability, and the final Cr and Ni contents (9.2% Cr, 3.22% Ni by weight) provided a composition favorable for martensitic transformation during the cooling process after FSW**[24].**

## IV. CONCLUSIONS

The results and discussions presented in the previous sections led to the following conclusions:

1. In all the welded joints, the profiles with the highest hardness correspond to the area of structural steel F82H and those with the lowest hardness correspond to 316L. The M3 joint presents the maximum peak (496 HV), located in zone F82H, 1mm to the left of the interface.
2. The increase in the speed of rotation and advance of the joint, have produced an increase in hardness in the welded joint, independent of the position of the dissimilar plates. The microhardness profiles are not symmetrical, even reversing the order of location of the dissimilar plates.
3. The maximum tensile values: YS(320 MPa), UTS (540 MPa), "ε" (17%) are presented in the M3 joint [ F82H (AS) – 316L (RS)]. The Modulus of Elasticity has remained almost constant, which means that the welding parameters (speed of rotation and advance) do not affect this property.
4. The maximum welding efficiency regarding mechanical resistance was 87%; corresponds to sample M3.
5. The maximum resistance to Charpy impact (27.5J) was obtained in the M3 sample, being slightly higher than the MB - F82H (26J) and lower than the MB - 316L (37J).
6. There was an exchange of materials around the zone (ST), produced by the material removal process, in addition to the diffusion process at the interface, due to the high friction temperature.
7. The microstructure in the zone (ST) of the joints showed: In the F82H zone mainly martensite and ferrite, and in the 316L zone it was totally austenite.

Finally, it is concluded that under the established welding parameters, the M3 sample obtained the best performance regarding hardness and mechanical properties in the joints welded by FSW.

## REFERENCES


[1]. S. Fukumoto, H.T subakino, K. Okita, M. Aritoshi, T. Tomita, Microstructure of friction Weld interface of 1050 aluminum to austenitic stainless steel, Mater. Sci. Technol.14(1998)333–338.

[2]. R.S. Mishra, Z.Y. Ma, Friction Stir Welding and Processing, Mater.Sci.Eng.R: Rep.50(2005)1–78.),

[3]. Shukla, R.K., P.K. Shah, 2010. Comparative study of friction stir welding and tungsten inert gas welding process. Indian Journal of Science and Technology, 3(6): 667-671.

[4]. Mishra, R.S., Z. Ma, 2005. Friction stir welding and processing. Materials Science and Engineering: R: Reports, 50(1): 1-78.

[5]. Nandan, R., T. DebRoy, H. Bhadeshia, 2008. Recent advances in friction-stir welding–process, weldment structure and properties. Progress in Materials Science, 53(6): 980-1023.

[6]. Arshad Noor Siddiquee, Sunil pandey, Noor Zaman Khan, Friction Stir Welding of austenitic stainless steel: a study on microstructure and effect of parameters on tensile strength, Materials Today: Proceedings 2 ( 2015 ) 1388 – 1397

[7]. Mishra R., Ma Z. (2005) Friction Stir Welding and processing. J Mater Science and Engineering 92:1-65.

[8]. P. Venkateswaran, A.P. Reynolds, "Factors affecting the properties of Friction Stir Welds between aluminum and magnesium alloys" Materials Science and Engineering A 545 (2012), pp.26– 37.

[9]. Metals & Alloys in the Unified Numbering System, 4th de., Society of Automotive Engineers, 1986

[10]. Zhu X K, Chao Y J. Numerical Simulation of Transient Temperature and Residual Stresses in Friction Stir Welding of 304L Stainless Steel [J]. J Mater Process Technol ,2004, 146(2): 263.

[11]. M.A. Mofid, A. Abdollah-zadeh, F. Malek Ghaini, "The effect of water cooling during dissimilar friction stir welding of Al alloy to Mg alloy" , Materials and Design 36 (2012), pp. 161–167.

[12]. S. Malarvizhi , V. Balasubramanian, "Influences of tool shoulder diameter to plate thickness ratio (D/T) on stir zone formation and tensile properties of friction stir welded dissimilar joints of AA6061 aluminum–AZ31B magnesium alloys", Materials and Design 40 (2012) , pp. 453–460.

[13]. C. Meran, V. Kov, A. Alptekin, Friction Stir Welding of AISI 304 Austenitic Stainless Steel, Mat.-wiss. u. Werkstofftech. 2007, 38, N° 10.

[14]. A.P. Reynolds, M. Posada, J. Deloach, M.J. Skinner, J. Halpin, T.J. Lienert, in: Proceedings of the Third International Symposium on Friction Stir Welding, Kobe, Japan, September 2001.

[15]. T.J. Lienert, W.L. Stellwag Jr., B.B. Grimmett, R.M. Warke, Weld. J. 2003, 82 (1), 1s.

[16]. P.J. Konkol, J.A. Mathers, R. Johnson, J.R. Pickens, in: Proceedings of the Third International Symposium on Friction Stir Welding, Kobe, Japan, September 2001.

[17]. C.J. Sterling, T.W. Nelson, C.D. Sorensen, R.J. Steel, S.M. Packer, in: K.V. Jata, M.W. Mahoney, R.S. Mishra, S.L. Semiatin, T. Lienert (Eds.), Friction Stir Welding and Processing II, TMS, 2003, pp. 165 – 171.

[18]. S.H.C. Park, Y.S. Sato, H. Kokawa, K. Okamoto, S. Hirano, M. Inagaki, Scripta Mater. 2003, 49, 1175.

[19]. R. Johnson, P.L. Threadgill, in: S.A. David, T. DebRoy, J.C. Lippold, H.B. Smartt, J.M. Vitek (Eds.),Proceedings of the Sixth International Conference on Trends in Welding Research, Pine Mountain, GA, ASM International, 2003, pp.88 – 92.

[20]. Avinish Tiwari , Piyush Singh, Pardeep Pankaj, Pankaj Biswas, Sachind. Kore, and Sukhomay Pal., Effect of Tool Offset and Rotational Speed in Dissimilar Friction Stir Welding of AISI 304 Stainless Steel and Mild Steel, Journal of Materials Engineering and Performance, JMEPEG ASM International doi: 10.1007/s11665-019-04362-y

[21]. D. Sunilkumar, Jithin Mathew, S. Muthukumaran, M. Vasudevan., Friction Stir Welding of 2.25Cr–1Mo Steel to AISI 316LN Stainless Steel, Trans Indian Inst Met, doi: 10.1007/s12666-020-01984-y
[22]. Guolin Guo and Yifu Shen, Microstructure and Mechanical Properties of Friction Stir Welded Austenitic-Ferritic Stainless Steels Using Staggered Joint Configuration, JMEPEG (2020) 29:5263–5272 ASM International, doi: 10.1007/s11665-020-05037-9
[23]. Cao , Tianyang Jiang , Wentao Hou , Guoqiang Huang , Yifu Shen , Yuquan Ding , Ping Shu., Effect of inhomogeneous fiber structure on the mechanical properties of friction stir welded SAF 2507 super duplex stainless steel, Materials Chemistry and Physics 283 (2022) 126026
[24]. H. Zhang, C.H. Zhang, Q. Wang, Effect of Ni content on stainless steel fabricated by laser melting deposition, Opt. Laser Technol. **101**, 363(2018)

Víctor Manuel Alcántara. "Friction Stir Welding in Austenitic 316L and Martensitic/Ferritic F82H Steels Joints: Effect on Mechanical Properties and Microstructure." *The International Journal of Engineering and Science (IJES)*, 12(1), (2023): pp. 12-21.